

SIRIO-2 L.A.S.S.O. MISSION: GEOSYNCHRONOUS  
SATELLITE LASER STATION RANGING-DATA ORBIT DETERMINATION SIMULATIONS

G. Vulpetti

TELESPAZIO S.p.a. per le Comunicazioni Spaciali,  
Rome, Italy

#### ABSTRACT

In this paper simulations of SIRIO-2 orbit determination are presented. They acquire a meaning because SIRIO-2 will be the first geosynchronous satellite for which a laser tracking is accomplished. This will take place through the LASSO mission, that is an intercontinental atomic-clock synchronization by using lasers. After an overview of the SIRIO-2 mission purposes and the foreseen characteristics of the laser ranging, a simulation scheme is developed to simulate the actual processing of high precision range values. By exploiting a recursive least-squares method and the prediction equations between observation sets, a sequential estimation equivalent to a Kalman-type filtering has been set up. It is shown how it is possible to reach quasi-steady state environments where the update S/C estimate is one order of magnitude better than an estimate from microwave-supported data such as the VHF's.

Keywords: orbit determination, batch and sequential estimation, least-squares estimate, prediction, filtering and smoothing.

#### 1. INTRODUCTION

European Space Agency shall launch a second satellite of the Italian SIRIO series, SIRIO-2, at the beginning of 1982. This spacecraft which is to be put into the stationary orbit, will be boosted at the Space Center of Kourou (French Guyana) by the European three-stage rocket ARIANE the upper stage of which will release SIRIO-2 in an elliptic transfer orbit. SIRIO-2 is equipped with its own Apogee Boost Motor which will be exploited for the geosynchronous station acquisition.

##### 1.2 Purpose of the Mission

SIRIO-2 will carry on-board a payload consisting essentially of two different pieces for two quite different purposes. The former one is related to the Meteorological Data Distribution (MDD) mission which should complement the ESA meteorological programme and improve the general performances of the Global Telecommunication System. The latter one is concerned with a scientific mission named Laser Synchronisation from Stationary Orbit (LASSO) designed for improving the current time-keeping accuracy. As a matter of fact, the uninterrupted demand for increasing both precision and accuracy in measurement of time has led to modern atomic

standards. Although extreme time precision is not a problem any more nowadays, however there is a lack of high-accuracy time dissemination, synchronisation and comparison between clocks over intercontinental distances.

On the other hand, scientific research, international telecommunications, Earth-based navigation and so forth (1) call for an increasing accuracy down to 1-2 nanosecond or better. The LASSO package carried by SIRIO-2 should allow several laser-plus-atomic-clock-equipped stations in Europe and USA to synchronize each other with a goal of one nanosecond. The geosynchronous orbit is exploited to operate over intercontinental distances in order to form a net of world-spread high-accuracy clocks.

##### 1.3 General profile of mission

Figure 1 shows the longitudinal section of SIRIO-2; in particular, the laser light reflector and the LASSO detectors at the bottom and near the center of the S/C respectively. The satellite will be initially placed at 25°W in order to be visible to both the American and European laser stations. After the first phase of the LASSO experiment, nominally six months, SIRIO-2 is to be moved to a new longitude station, 20°E, to perform MDD mission for a foreseen duration of 18 months. The respective coverage zones are displayed in Figure 2. The overall mission time (2 years) may be differently shared between LASSO and MDD while the former task is in progress.

#### 2. THE LASSO EXPERIMENT

TELESPAZIO will perform the twofold task of SIRIO Orbit Control Center (SIOCC) and LASSO Coordination Center (LCC). Here we do not detail the LASSO experiment policy and its technical specifications which can be found in ref. 2; rather, we emphasise those aspects relevant to orbit determination. The scenario is that officially presented by TELESPAZIO and accepted by ESA.

The LASSO experiment operational principle is synthesised in Figure 3. Two (or more) ground stations endowed with both high-power pulsed lasers and atomic clocks laser, at pre-established instants, toward SIRIO-2.

The pulse departure times are measured and recorded in the respective time scales. Light pulses strike the satellite which is equipped with a highly-stable clock measuring the time



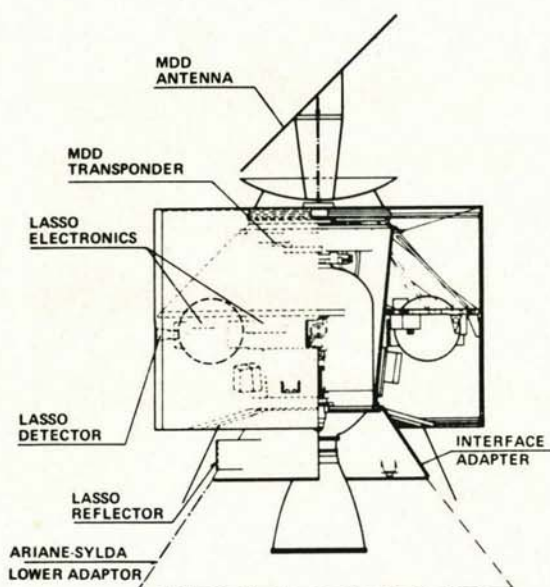


Figure 1. SIRIO-2 axial section

difference of the arrival of the pulses. These data are relayed to Earth by S/C telemetry. The corner reflector on-board sends a part of the wave packet energy back to stations. A flux of a few photons per square meters is collected by the station's telescope which focalises them onto a highly sensitive and fast photo-detector and the clock measures the return time. As one can easily recognise, this is a modern version of the synchronization method proposed by Einstein. Any couple of stations and the S/C are characterised by six measurements of time. Figure 3 gives the

basic relation to synchronize two stations through the experimental time shift  $C$  so determined. Naturally, Earth rotation, S/C radial velocity and relativistic corrections are to be taken into account.

One of the main immediate outcomes from such an optical S/C tracking is represented by range, which is indirectly measured as soon as the round-way time is known. Associating this value with the right S/C GMT is actually an iterative procedure inasmuch as the uplink and downlink propagation distances are different in value and the time at which a pulse is received by S/C is not directly known, on-board clock being able to correctly sense time differences. (These last calculations are imbedded in a preprocessing phase during operational environments).

It is clear that several stations participating the LASSO experiment can get at sets of high-precision ranging data which could be used to improve the SIRIO-2 trajectory determination. As a feedback, the information gained about the satellite can be, in turn, exploited for better computing the laser pointing angles which LCC must disseminate to the stations. A further important improvement from a precise S/C state estimation consists of determining the arrival pulse time window for each attending station. This in order to detect as low spurious pulses as possible in number, although a narrow-band filter is also used at telescope. Such window translates the a-priori uncertainty in the S/C position along the station's line of view. Figure 4 displays this situation. The indetermination along the vector radius from station to S/C is delimited by the planes tangent to the satellite position error ellipsoid and orthogonal to the mentioned radius. LCC provides such a value at the beginning of every LASSO session. Thus the performance of a scientific experiment (such as LASSO) and the opportunity of greatly improving the S/C state in a stationary orbit are problems interlacing each other.

It is in this light that the results of the simu-

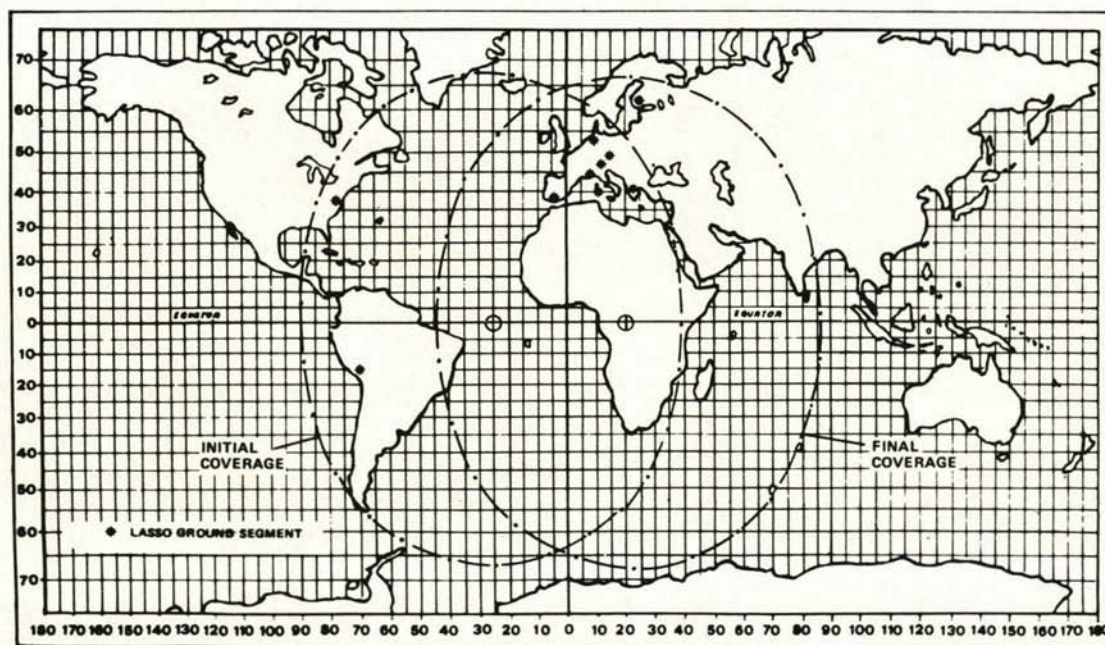


Figure 2. SIRIO-2 coverage zones for LASSO and MDD missions.



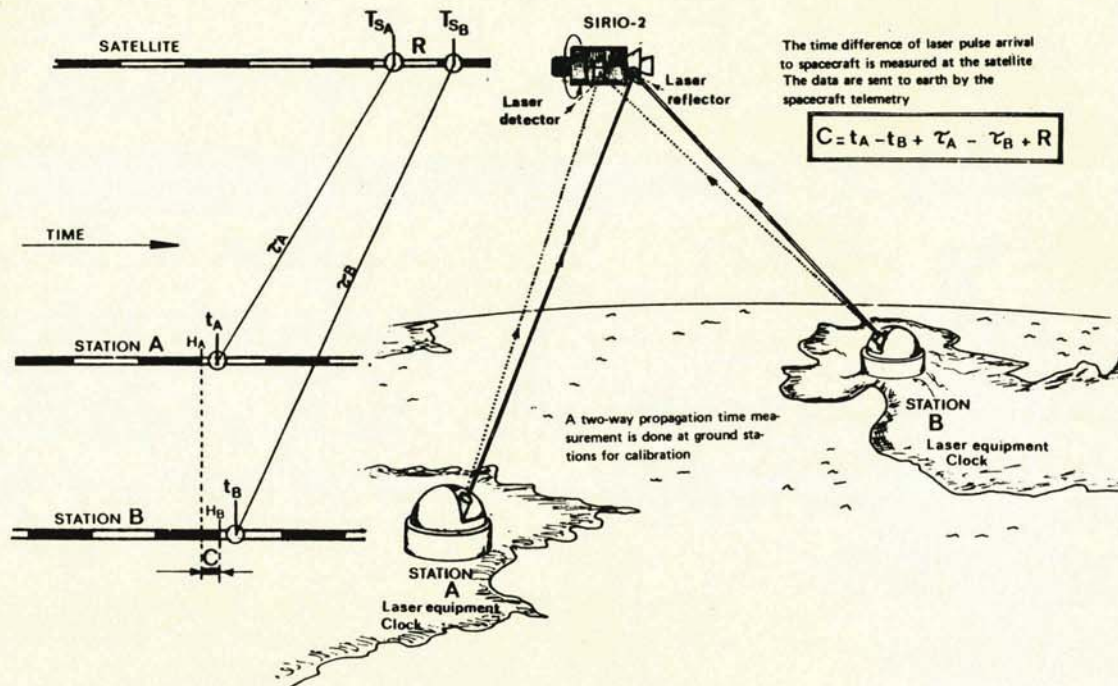


Figure 3. Principle of synchronisation between two laser-and-atomic-clock-equipped stations. The value of  $C$  allow stations to synchronise each other.

lation discussed in this paper should be viewed.

### 2.1 General LASSO constraints

The current profile of the LASSO experiment consists of sessions lasting one hour within which not more than six participating stations can usefully lase to SIRIO-2. Each session, in turn, is subdivided in sequences of firing of about 5 minutes separated by intervals of some minutes. In every sequence each station can lase at a prefixed frequency by starting from a sequence-dependent time in order to get first or lower order resonance with the SIRIO-2 rotation frequency. In our simulations we have assumed a session of six five-minute sequences separated by five six-minute intervals during which resetting of the instruments is made in a station.

A maximum of five stations has been considered here. Moreover, because to lase successfully to SIRIO-2 depends strongly upon weather, instrument failure or other contingency, a selection is made according to certain criteria in order to simulate these environments. The ultimate consequence here is merely not to process certain sets of range data.

Also of concern in the LASSO experiment is the frequency of the sessions. Currently, not more than 2 sessions per week are scheduled, although special sessions devoted exclusively to ranging are planned. In our simulations no special session has been considered.

According to the current plans at first four stations are european and one is american. Finally we have supposed that only one range value per minute and station is useful for processing. (This, perhaps restrictive, condition may be in reality modified when the first actual sets of LASSO data are processed).

### 3. THE SIMULATION SCHEME

Orbit determination by SIOCC is not exclusively based on the LASSO experiment. In fact, trajectory estimation through LASSO must be primed and, if SIOCC lacks LASSO ranges, successive LASSO sessions must be prepared by LCC (to within its duties). In any case, SIRIO-2 has to be tracked independently of LASSO. ESA will perform tracking through its VHF stations of Redu, Kourou and (probably) Malindi. Such stations will supply SIOCC with range data on a regular weekly basis. These data are to be processed for estimating the SIRIO-2 orbital elements. Such regular phase has been included in our general simulation scheme, primarily for having a good reference orbit for processing LASSO data. Figure 5 shows the flow-chart of this simulation step. In the trajectory propagation block a reference geosynchronous orbit is computed over a specified time span. A file (orbit data file) containing the related S/C acceleration history is generated. It represents the main input to the Observation Simulation block which also requires station-dependent data, ob-

servation noise (a white sequence), observation frequency and so forth. All this results in a file of simulated observations of VHF range from the ESA stations. In the last block, the Orbital State Estimation, this sample of data is processed by means of a differential correction least-squares batch estimator by starting from a rough initial guess of S/C state and covariance matrix at

a certain epoch. Also guessed are the noise and the biases observations (ignoring the respective levels inserted into the simulator, of course). The main outcome from such scheme is a sufficiently-precise estimate of the SIRIO-2 S/C at epoch. State and error covariance at the specified time will prime the more complex LASSO data processing we will discuss later.

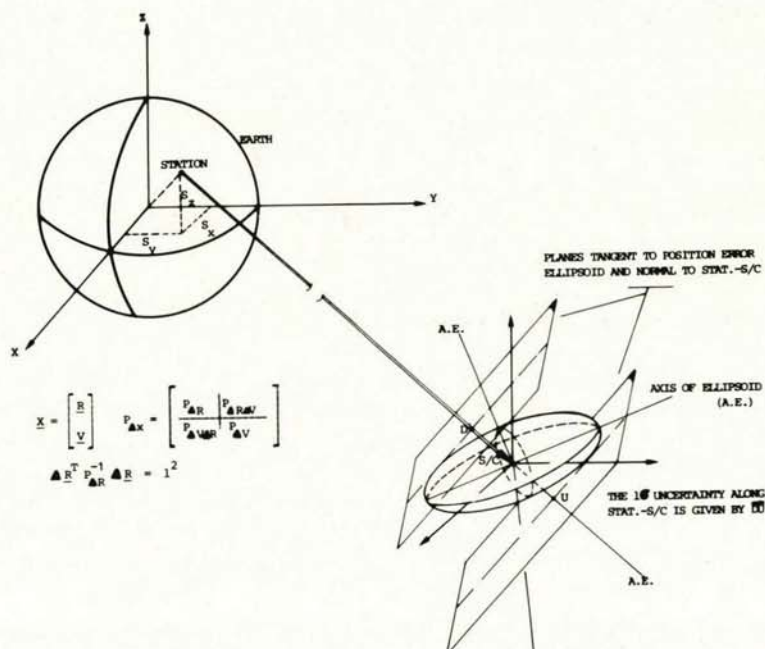


Figure 4. 1- $\sigma$  uncertainty in S/C position only along the line of sight station-satellite. This value intervenes in setting a time window to the return laser pulse.

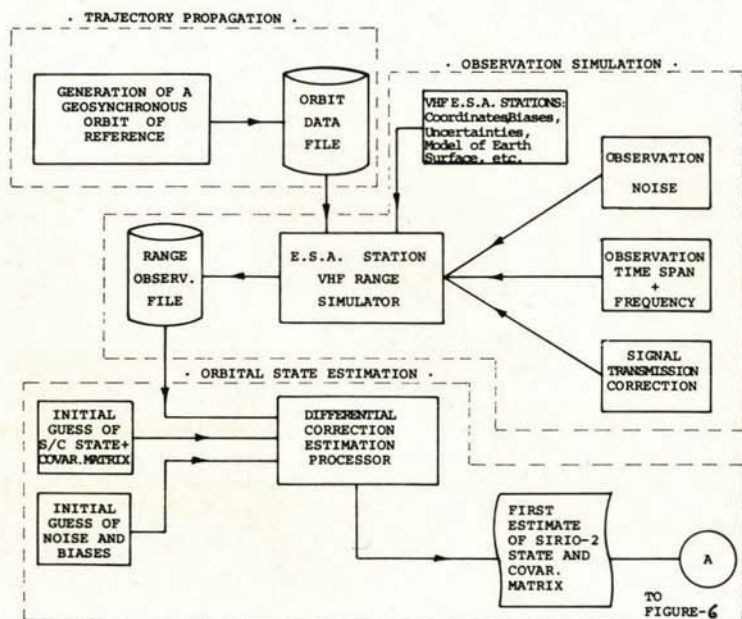


Figure 5. Scheme of simulation of VHF ranging data processing.



### 3.1 Reference Trajectory Characteristics

The reference orbit model is taken the same for both the VHF range and LASSO range processing. The Earth gravitational field assumed here is based on the harmonics as given in a NASA/Coddard Space Flight Center model (GEM-9).

Zonal-tesseral-sectorial harmonics up to seven degree and seven order have been included in the computation, whereas Sun and Moon perturbations have been added. Furthermore, the effect from solar radiation pressure and polar motion have been considered. A true-of-date reference frame is the basic reference system throughout all calculations. The date is moved forward when required. All equations are numerically integrated by a 8-order fixed step cowell predictor-corrector system with either a 8-order Runge Kutta or an iterative method as starter. Numerical stability and regularity of the state variables are assured. Analogous properties hold for the propagation system used during the estimation process, namely, when the variant-orbit equations are to be integrated.

### 3.2 Astronomical Pointing Angles

The LASSO experiment represents a quite new methodology to be tested and developed essentially because a reflector as far as a synchronous satellite is used. In addition, the nature of the experiment is rather complex. Therefore, it is not excluded that in the early phase of LASSO precise measurements of range are not available in a sufficient number or certain stations fail to track SIRIO-2 for any reason. This may occur even in an advanced phase of the experiment too.

Moreover, it can be of great interest to further improve the S/C state estimation and/or to precisely estimate other non-state variables. All this could be achieved fairly if the ranging data were complemented by angular data (e.g. azimuth and elevation) of sufficient low noise. A way could be to utilise the laser pointing angles for those pulses actually striking SIRIO-2. It would be quite simple to collect them, but the main drawback should consist of a lower limit in the associate noise in as much as we cannot know in which point of the pulse wave front broad disk the corner mirror reflects light. Another aid could come from astronomical observations, especially in time intervals close to the autumn and spring equinoxes. Such angular data are expected to be very low noisy by exploiting modern techniques in astronomy.

If the Sun-declination reflection is exploited, the useful visibility window from a single observatory is rather narrow (a few days); however, as soon as a net of telescopes are available (for SIRIO-2 mission) in Europe and America, we can have observations spanned over some weeks at least.

The Astronomical option is considered in this paper, all the more SIRIO-1 has been already successfully tracked by telescopes in Europe.

### 3.3 High-Precision Processing Simulation Scheme

Figure 6 displays the block diagram of trajectory Propagation, Observation Simulation and S/C Orbit Determination employed here to simulate the

environments previously described and the ensuing processing. Whereas the general policy is similar to that of Fig. 5, in the current case two observation files are generated containing laser tracking data and astronomical pointing angles respectively, according to the LASSO constraints and the intervals of visibility from the chosen observatories. A data selection block simulates real environments by discarding/accepting observations on a basis of station, observation type, time span and observation frequency. During processing both a dynamical weight and the so-called "consider" variables (see next section) are taken into account. The main output consist of S/C state, error covariance matrix and residual information, optionally on a graphic device.

## 4. PREDICTION/UPDATE ESTIMATION POLICY

In this section we expose the system and measurement models together with the policy of estimation employed here. The central point consists of simulating the evolution of the precision of the SIRIO-2 state according to the overall information available to us at this moment and by means of an already-working estimator in TELESPAZIO. In other words, we do not perform a design analysis in order to modify our current processing system, but use its extreme performance to gain information about the possible improvement of the S/C state through high-precision measures.

Here we shall not give the theory of the estimation process we have used. Only the fundamentals are repeated for clarity. Extensive and complete aspects of our estimation procedure, both theoretical and practical, can be found in Refs. 3,4,5.

### 4.1 State and Measurement Models

Let us denote by  $X(t)$  the six-component cartesian vector and by  $Z(t)$  the observation vector at time  $t$ . At first we shall treat both system and measurement model as continuous even though only discrete samples of data are processed.

The S/C state evolution is assumed to be governed by the following stochastic differential vector equation:

$$dX(t) = s(X,t) dt + G(t) d\beta(t) \quad (1)$$

where  $\beta(t)$  is a vector Brownian motion process with the following statistics

$$E(d\beta) = 0, E(d\beta d\beta^T) = Q(t) dt \quad (2)$$

where  $E(\cdot)$  denotes the expectation operator and  $Q$  is the spectral density function of the process.

The matrix  $G$  is a multiplying matrix in the driving term. In our model (in simulation environments) the only state noise source comes from computer roundoff. Therefore  $G$  is rather small. The process  $\beta(t)$  and  $X_0 \sim N(\hat{x}_0, P_0)$  are assumed independent,  $\hat{x}_0$  being the state estimate and  $P_0$  its covariance at  $t_0$ .

The vector function  $s(X, t)$  contains the central



force and the perturbations described in sect. 3.1.

The observation model is given by the following stochastic equation

$$dZ(t) = f(x, y) dt + d\gamma(t) \quad (3)$$

where  $\gamma(t)$  is another brownian motion process, by independent of  $\beta(t)$ . Its statistics is

$$E(d\gamma(t)) = 0, E(d\gamma d\gamma^T) = R dt, R > 0 \quad (4)$$

The main source of uncertainty in our LASSO processing simulation comes from the driving term in Eqs. 3. Also,  $\hat{x}_0$  does not depend upon  $\gamma(t)$  and viceversa. In Eqs. 3 there is a vector denoted by  $y$  which represents the set of those quantities of which one has an estimate a-priori, but generally they are not required to be re-estimated. However their importance consists of augmenting the S/C state covariance inasmuch as they intervene only through their uncertainties. They are called "consider" variables (CVS) in contrast to the "solve-for" variables (SVS). Nevertheless during preprocessing some of the CVS could be estimated as part of SVS for improving their precisions; but in successive runs they re-enter the CVS and their updated standard deviations (and the new estimated values, of course) affect the proper S/C state estimate.

We suppose that the initial estimate of  $y_0$ , say  $\hat{y}_0$ , are uncorrelated with both  $\hat{x}_0$  and  $\gamma$  primarily because an a-priori correlation matrix of such type is usually unavailable.

In our basic estimation procedure (the recursive least-squares method employed in a mixed sequential-batch policy as we shall see) we will use the linearised form of Eqs. 3 in "passing" from a trajectory to another sufficiently close to the previous one.

If we consider deviations rather than absolute quantities, we have

$$\Delta Z(t) = M(X, y_0) \Delta X + N(X, y_0) \Delta Y_0 + n \quad (5)$$

where the matrices  $M$  and  $N$  are defined by

$$M = \frac{\partial f(X, y_0)}{\partial X}, \quad N = \frac{\partial f(X, y_0)}{\partial y} \quad (6)$$

and we have set  $d\gamma/dt = n$ , (formally) a white noise.

Similarly, the system model linearisation yields

$$\frac{d}{dt} (\Delta X(t)) = S(X, t) \Delta X(t) + G(t)w \quad (7)$$

where  $w$  is the white noise "associated" with  $\beta(t)$ .

Naturally,  $S(X, t) = \partial s(X, t) / \partial X$ .

In Eqs. 5, 7 the increments are to be intended with respect to the current nominal or reference trajectory (generated without noise).

#### 4.2 Mean and Covariance of the Measurement residuals

Remembering the statistics of the white noise, the meaning of the CVS and the assumptions made about them, we have:

$$E(\Delta Z) = E(M \Delta X) = 0 \quad (8)$$

taking into account Eq. 7 and the fact that the obvious choice of the reference trajectory is made starting with  $X_0 = \hat{x}_0$ .

From Eq. 8 and the definition of (auto) covariance matrix, we obtain

$$P_{\Delta Z} = M P_{\Delta X} M^T + N P_{\Delta Y_0} N^T + R + C \quad (9)$$

where  $P(\cdot)$  denotes the covariance matrix of  $(\cdot)$  and the superscript  $T$  does matrix transposition. Note in Eq. 9 that the variance-covariance set of the CVS is not updated for the current trajectory. The matrix  $C$  contains the cross-covariance terms, that is

$$C = M C_{\Delta X \Delta Y_0} N^T + N C_{\Delta Y_0 \Delta X} M^T \quad (10)$$

where  $C(\cdot)$  represents the cross-covariance matrix of  $(\cdot)$  in the order.

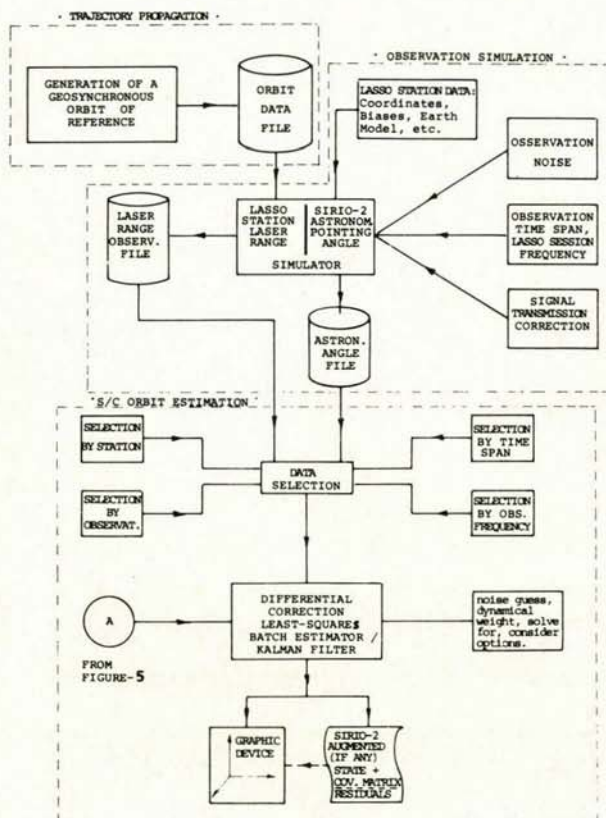


Figure 6. Sequence of simulation steps employed for LASSO ranging and astronomical pointing angle (if any) data processing in SIRIO-2 orbit determination.

#### 4.3 Mean and Covariance of the State

The best estimate of the state can be found by



solving the following variational problem:  
minimise the loss function

$$J = \frac{1}{2} \int_{t_0}^t \Delta Z^T R^{-1} \Delta Z d\tau + \frac{1}{2} \int_{t_0}^t W^T Q^{-1} W d\tau + \frac{1}{2} \Delta X_0^T P_0^{-1} \Delta X_0 \quad (11)$$

with respect to  $\Delta X$  and  $W$ , subject to the differential constraint given by Eq. 7. Such continuous least-squares problem can be solved by either invoking the "weak" form of Pontryagin's minimum principle or using classical variational techniques.

The solution for  $\Delta X(t)$  is given by a differential equation:

$$d\Delta \hat{x}(t)/dt = S(x, t) \Delta \hat{x}(t) + K(x, t) \Delta Z(t) \quad (12)$$

with the initial condition  $\Delta \hat{x}(t_0) = 0$ . It can be shown (refs. 3, 4, 5) that the covariance matrix of the deviation  $\Delta X(t)$  satisfies the following Riccati equation

$$\dot{P}_{\Delta x} = S P_{\Delta x} + P_{\Delta x} S^T + Q Q^T - K K^T \quad (13)$$

with  $P = P_0$  as initial condition

In Eqs. 12, 13 the matrix  $K$  is given by

$$K = P M^T R^{-1} \quad (13a)$$

(because no correlation has been supposed between  $w$  and  $n$ ).

Notice how, having interpreted  $n$  and  $w$  in Eqs. 5, 7 (or  $\beta$  and  $\gamma$  in Eqs. 1, 3) on a probabilistic basis, the continuous least-squares problem is quite equivalent to a Kalman-type filtering for driving terms consisting of uncorrelated white noises. Complete observability is assumed as well.

#### 4.4 Discretisation

As we shall see in the next section, the overall estimation procedure consists of several batches of observations processed separately; between them S/C state and error covariance matrix evolve and their respective predictions are made at the time when a new set of measurements are available. Such prediction/update sequence represents the way SIOCC will process LASSO ranging and astronomical pointing angle (if any) data. Each observation batch is analysed by means of a recursive least-squares solution so that a discretisation of the above basic theoretical filtering is necessary. For the sake of simplicity, the term  $Gw$  is neglected. In contrast, we retain the "constraint" on the initial satellite state. Thus, the second integral in (11) disappears whereas the first one reduces to a summation. Reformulating the problem by expliciting the S/C state estimate on the first reference orbit, passing from  $j$ -th orbit to the  $(j+1)$ -th one we obtain

$$\Delta \hat{x}_{j+1} = (M_j^T R^{-1} M_j + P_0^{-1})^{-1} (M_j^T R^{-1} \Delta Z_j + P_0^{-1} \Delta \hat{x}_{0j}) \quad (14)$$

where we have set  $\Delta \hat{x}_{0j} = x_0 - \hat{x}_j = \Delta \hat{x}_{0,j-1} - \Delta \hat{x}_j$ . Note that the expectation of  $\Delta \hat{x}_{0j}$  is zero. The error covariance matrix is then written as

$$P_{\Delta x, j+1} = E((\hat{x}_{j+1} - x)(\hat{x}_{j+1} - x)^T) = E((\Delta \hat{x}_{j+1} - \Delta x_j^*)(\Delta \hat{x}_{j+1} - \Delta x_j^*)^T) \quad (15)$$

where  $\Delta x_j^*$  represents the departure of the "true" orbit from the  $j$ -th estimated orbit, namely,  $\bar{x} - \hat{x}_j$ .

(For the sake of simplicity we drop the subscript  $j$  because no confusion arises from what will follow). At this point we can use the results of sect. 4.2 for saying more about Eqs. 14, 15. Setting  $(M^T R^{-1} M + P_0^{-1})^{-1} = H$ , we have

$$E(\Delta \hat{x}) = H(M^T R^{-1} E(\Delta Z) + P_0^{-1} E(\Delta \hat{x}_0)) = 0 \quad (16)$$

The best estimate given by Eq. 14 is then unbiased.

The general expression for  $P_{\Delta x}$  is quite complicated. If we suppose to process a sufficiently high number of measurements and fix our attention on the converged trajectory, we found the following final expression for the state error covariance matrix.

$$P_{\Delta x} = (I + H M^T R^{-1} N P_{\Delta y_0} N^T R^{-1} M + C^* + C^{*T}) H \quad (17)$$

where  $C^* = C_{\Delta x \Delta y_0} N^T R^{-1} M$  and  $I$  is the 6-dimension identity matrix.

Details about Eq. 17 can be found in Ref. 6.

Eq. 17 can be further simplified after noting that, if  $\Delta X(t)$  and  $\Delta y_0$  are initially uncorrelated as we have supposed, they will remain as such during the filtering process. Therefore  $C^* = 0$  and Eq. 17 results in

$$P_{\Delta x} = (I + H M^T R^{-1} N P_{\Delta y_0} N^T R^{-1} M) H \quad (18)$$

Eq. 18 is our covariance matrix at convergence.

Let us note, however, that the cross-covariance  $C_{\Delta x \Delta y}$  is not zero in general. In fact we deduce from Eq. 18.

$$C_{\Delta x \Delta y} = -H M^T R^{-1} N P_{\Delta y_0} \quad (19)$$

Let us point out that, in the case of no CVS, the solution of Eq. 18 is the function  $H$  itself. Therefore, combining Eqs. 18, 19 we get

$$P_{\Delta x} - H = -C_{\Delta x \Delta y} N^T R^{-1} M H \quad (20)$$

Although not numerically employed, Eq. 20 tells us how it is important to take into account small sources of uncertainties when very precise measurements are to be processed, as in the case of the LASSO experiment's.

#### 5. DISCUSSION OF THE RESULTS.

The previous prediction and updating process has been applied to a 24-day interval of the synchronous orbit of SIRIO-2, namely from Feb. 28 to 23 March 1982.

During this time it is assumed that both LASSO experiment is being begun and astronomical obser-



vations from northern observatories are performed (the S/C is in a nearly equatorial orbit and the Sun's declination is negative ranging from  $-9^\circ$  to  $0^\circ$ ). The number of stations trying a synchronisation is assumed to be five, namely, the stations of the commissioning phase (according to the current preliminary development and scheduling) and one U.S. station: KOOTWIJK (Netherlands), WETTZELL (West Germany), GRASSE (France), SAN FERNANDO (Spain) and GODDARD SPACE FLIGHT CENTER (Maryland, U.S.A.). (We make no distinction between the two possible companies responsible for this station that is, NASA or University of Maryland. We have only indicated the location of the station). As far as the precision foreseen for the LASSO ranging data, it depends essentially upon the length of the laser pulse, a random time bias due to the double travel of the laser light through the atmosphere, the uncertainty with which the coordinates of a station are known in an Earth-centred inertial frame, the number of photoelectrons actually detected and the current uncertainty about the speed of light.

The laser pulse width of the mentioned stations varies from 0.1 ns to 10 ns (1 ns = 1 nanosecond). In ref. 7 authors assert that, once an atmospheric travel correction is made by local pressure, temperature and humidity measurements, there would remain a "residual" of imprecision of 0.5 ns at most. Currently, Doppler campaigns permit

obtaining the x, y, z components of the position of a station with the precision of the order of 1 meter.

Since one of the above stations is not given with such a measurement campaign, we have assumed a maximum of 10 meters in the 1- $\sigma$  precision for those stations. (Furthermore, it must be considered that some new station can enter the initial LASSO Working Group and such station may not have been yet included in a Doppler Campaign).

The photodetectors which are placed downstream from the laser station's telescope are able to reveal an amount as low as two photoelectrons from the return pulse. Unfortunately, the total intensity of this pulse is not much more than this limit whereupon it should be difficult or impossible to establish the "barycenter" of the profile of the received light.

Finally, in order to process ranges one must convert the travel time through the speed of light which is known with 0.004 parts per million, or 1.2 meters.

The above uncertainty budget (station location excluded) amounts to about 3 meters at most. We have considered an a-priori noise varying from 1.5 to 3 meters in generating a file of simulated laser range observations. The imprecision of the tracking station locations has been added and successively considered in the estimation algorithm through the mechanism of the above mentioned

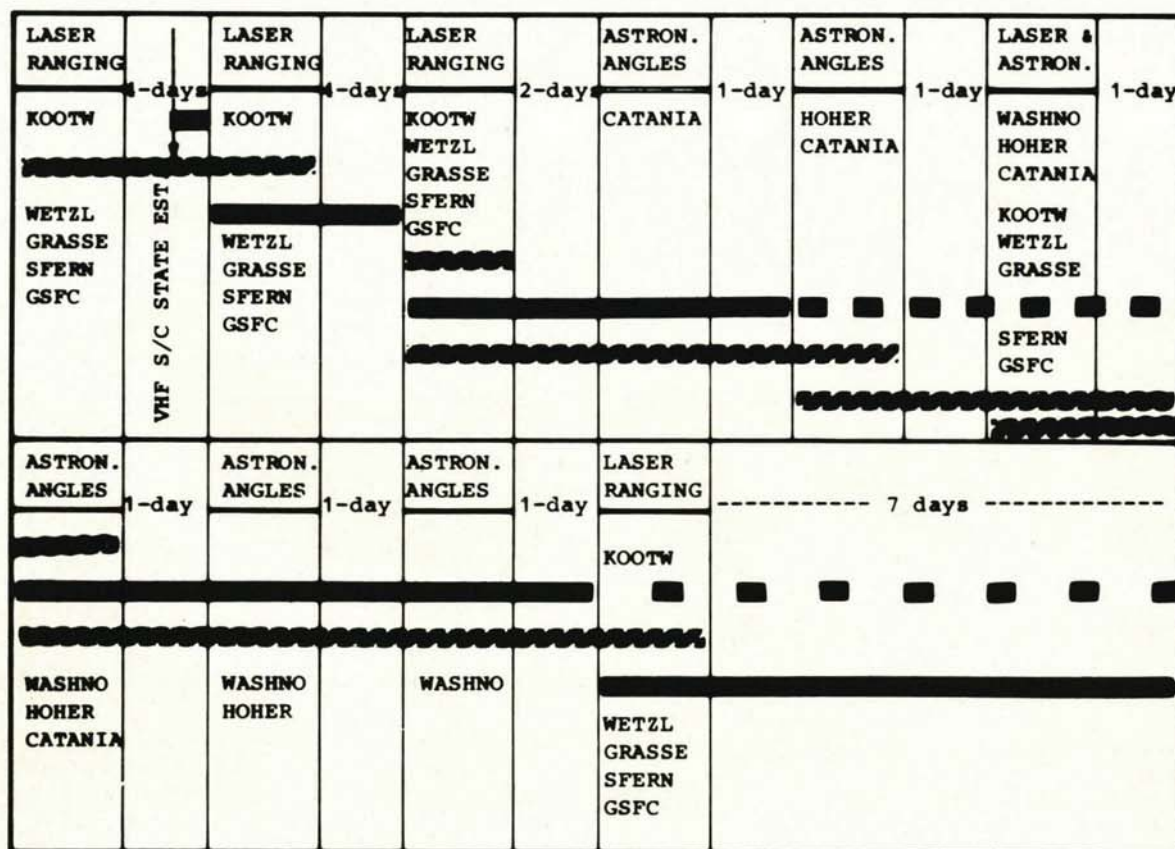


Figure 7. Sequence of processed observation sets for updating S/C orbital elements after propagation (see text for explanation).



"consider variables". Possible biases of detection with related standard deviations fall to within the CVS; their initial guesses and updated values have been inserted into the overall procedure of estimation. Also, inputting the noise matrix  $R$  a dynamical weighting function of the laser elevation angle has been introduced.

As far as the astronomical pointing angles are concerned, we have chosen (only for purpose of simulation) three observatories: CATANIA (Italy), HOHER LIST (West Germany) and WASHINGTON NAVAL OBSERVATORY (U.S.A.). Noise has been assumed to be as low as 2-3 seconds of arc. Station location errors, although less important than in the LASSO ranging, have been considered in a quite similar way.

Acronyms of both the laser stations and observatories have been used in Fig. 7 which shows the sequence of the observation sets, the involved stations and the time spans taken into considerations. The black strips represent the intervals of prediction; the slashed strips do the observations-included spans employed to update the S/C state and covariance after a prediction. The "dashed" black strips regard a continuation of prediction in the (not impossible) case certain new sets of measurements were actually unavailable by some failure or other contingency.

Processing the indicated batches of (range and/or pointing angle) observations can be thought as equivalent (for our purposes) to a memory-limited filter plus a lag-fixed smoothing (3, 4).

The results we are going to discuss are substantially independent of the level noise in the range considered above.

Figure 8 displays the time behaviour of the root-mean-square (rms) of the predicted / updated S/C position error cartesian components. For plain graphical reasons the y and z components have been right-shifted with respect to the x-component.

Also plotted are the standard deviations of the S/C vector radius magnitude, the osculating semi-major axis and longitude.

The starting point is the VHF estimate which is about 750 m in the Z-axis (or about  $10^{-1}$  deg in orbital inclination); the indeterminations on the other axes are well beyond 100 m. After a short initial propagation, the rms are updated by exploiting the first data coming from two LASSO sessions. This results in a considerable improvement of the rms, especially in x and y axes, which fall down below 100 meters whereas the estimation in the north-south direction is still relatively poor.

Notice that from an uncertainty such as VHF's one LASSO session is not sufficient to assure a good convergence. Successively, the overall information gained so is degraded until the next LASSO session is performed after four days. And so forth, by exploiting both LASSO sessions and astronomical "sessions".

(The dashed lines correspond to the dashed black strips of Figure 7). We see that the first updates are limited by the z-uncertainty.

Successively, because during propagation such component decreases (the overall error in position augments, of course), about 10 days from epoch, the y-component prevails over both the

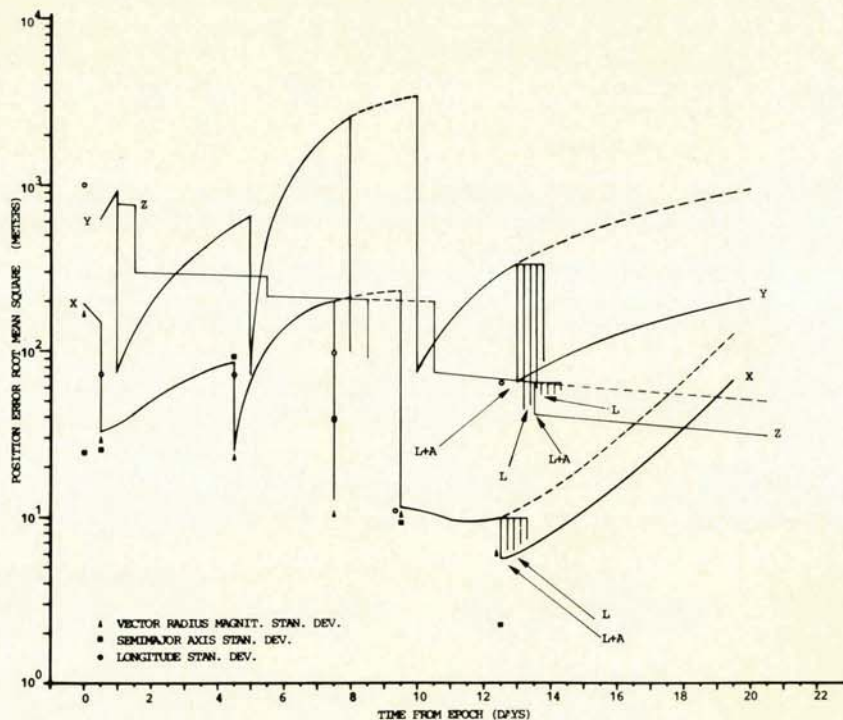


Figure 8. S/C position error root mean square time evaluation. The cartesian components are shifted each other for clarity.



other components and bounds the precision. In contrast, the x-component achieves values below 10 and 100 meters at the last update and prediction respectively. It is meaningful that after the last 7-day propagation, the most precise information concerns the orbit inclination. This must be ascribed to the stabilizing effect of the first two terms in the right-hand side of Eq. 13, the system noise being negligible as said above. In general, these alternances of error amplification by propagation and its reduction by data processing show that a quasi-steady state is reached, the ultimate precision being limited largely by the combination of the observation noise and the station location precision. By this regard it is noticeable to compare laser-only data processing with laser-plus-astronomical data processing. Five values for each cartesian component are displayed after 12.5 days from epoch (the vertical straight lines are shifted for clarity). Four sets of laser range (denoted by L), obtained by rejecting one LASSO station of the five chosen and varying the total number of ranges from 96 to 360, are to be compared with the maximum possible number of observations (546) usable at this time (denoted by L + A). Apart from 2 cases for the y-component, the L processing is worse than the L + A updating especially as far as the z-component is concerned for which an improvement of 30% can be achieved.

The astronomical angle aid can be better visualized by noting the jump-down in all the components after 9.5 from epoch, when the third update was supposed to fail for simulating some actual contingency. The alternative update has resulted to be the strongest one, all the more that a further propagation would become necessary as shown by the first dashed curved lines in Figure 8.

In this phase we have obtained a mean of the

range residuals varying from 35 to 40 m whereas angles display a mean of 3-4 arcseconds.

Such values show in a quantitative manner how much range measurements are affected by the SI-RIO-2 elevation-low station location uncertainties, whilst angles remain practically unaffected.

This seems to be the extreme precision for the S/C position reachable under the assumptions made here.

A further information is contained in Figure 8. The uncertainty in the vector radius magnitude draws near the highest precision component's. The error in longitude is practically unchanged (70-80 m) after the first update.

Finally, the semimajor axis shows a dispersion less than 3 meters at the final update, about one order of magnitude with respect to the VHF estimate. The general behaviour of these physical quantities is easily foreseeable inasmuch as slow parameters.

Quite similar considerations can be made about the rms of the velocity error components the time-behaviours of which are graphed in Figure 9. Maximum precision pertains to the y-component that can be as low as  $5 \times 10^{-2}$  cm/s.

In contrast, x and z components bound the precision by an order of magnitude at the last update, while they equal each other after 4.5 days namely  $\approx 1$  cm/s.

The rms of the radial velocity error along the station-S/C line of view can be computed in a way similar to that done in Fig. 4. (Naturally, when a probability is assigned for obtaining certain  $\delta r$  and  $\delta v$  intervals simultaneously, the whole covariance matrix must be considered).

Finally, Figure 10 displays the maximum rms in position and velocity error as function of the total number of observations processed. Values are normalized on the corresponding VHF estimates. The general properties noticed before appear

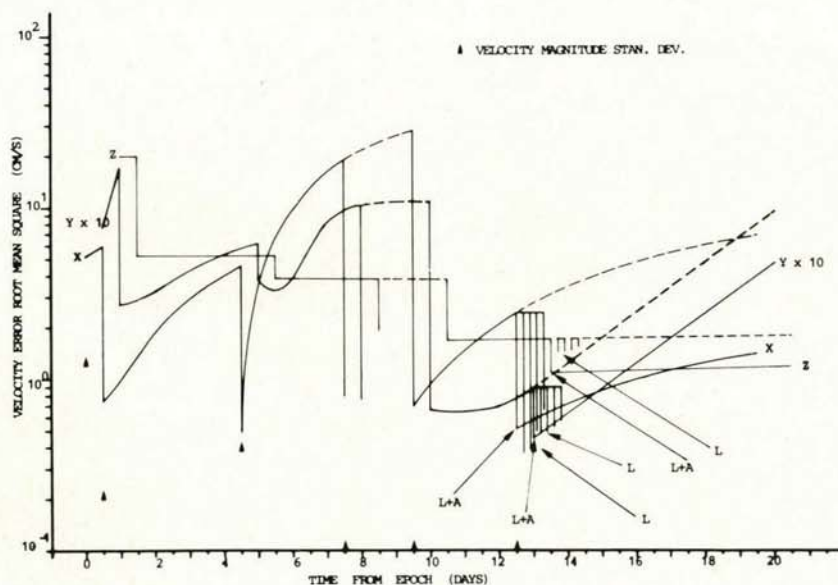


Figure 9. S/C velocity error root mean square time evolution. The cartesian components are shifted each other for clarity.



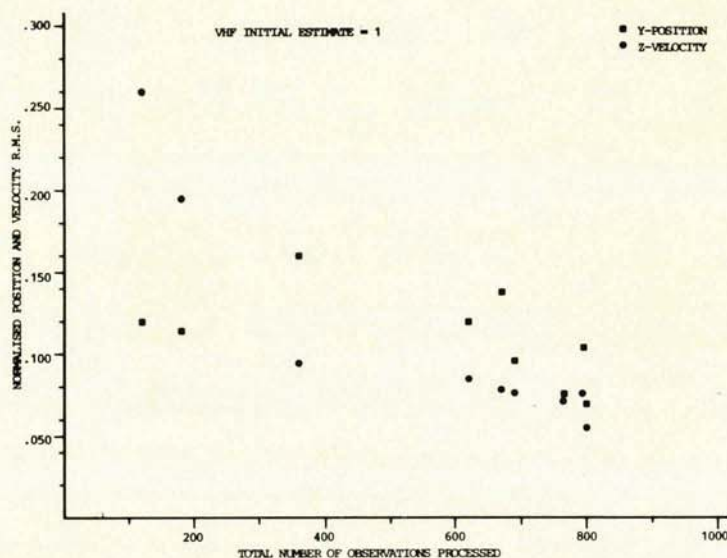


Figure 10. Minimum precision root mean square of position and velocity error vs the total number of observation processed. The normalisation is with respect to the VHF estimate.

evident again. In particular, in near steady-state conditions 800 measurements of range, azimuth and elevation spanned over almost two weeks are necessary to improve the VHF estimates (both position and velocity) by more than one order of magnitude. However, one should keep in mind that such a happy situation - a "crowd" of laser and astronomical observations of different types - will be rather rare, except during weeks near the equinoxes, provided that the Sun-declination reflection is exploited.

#### 6. CONCLUSIONS

A predicted/updated estimation procedure equivalent to a Kalman-type filtering driven by white noise has been set up for simulating the actual processing of high-precision laser ranging data for orbit determination (and, optionally, high-precision astronomical pointing angles) within the LASSO mission. In particular, a time span of 24-day near the equinox of spring 1982 where both LASSO sessions and astronomical observations could be performed.

Analysing the root mean squares of the cartesian components of the estimated error in position and velocity as function of time and the number of observations, an almost steady-state can be reached. In such environments, by processing periodical sets of some hundreds of (2-3)-meter-noisy range values, one can achieve a precision one order of magnitude better than a VHF - based estimation. Moreover, it has been noticed that the above precision can be either kept or slightly improved by adding astronomical angle data (e.g. azimuth and elevation) in the processing especially if some LASSO session fails for any reason.

#### 7. REFERENCES

- 1). Melbourne W G, Navigation between the planets, Scientific American, 1976, No 7, pp. 59-74.
- 2). Coffaro P, Palutan F and De Agostini A, LASSO Coordination Center (LCC) Analytical and Technical Specification, TELESPIAZIO, DPS-TES-ST-1412.01/191280.
- 3). Jazwinski A H, Stochastic Process and Filtering Theory, Academic Press, New York 1970, x-y.
- 4). Gelb A et al, Applied Optimal Estimation, The M.I.T. Press, Cambridge, Mass. 1974, x-y.
- 5). Maybeck P S, Stochastic Models, Estimation and Control, (Vol. I), Academic Press, New York 1979, x-y.
- 6). Cappellari J O et al, Mathematical Theory of the Goddard Trajectory Determination System, NASA/GSFC X-582-76-77, Maryland, April 1976.
- 7). Alley C O et al, Laser Ranging Retro Reflector: Continuing Measurements and Expected Results, SCIENCE Jan. 1970, 167 pp 458-460.

#### ACKNOWLEDGEMENT

The author is grateful to Mr. D. Azzaro of TELESPIAZIO who has suggested using astronomical angles for SIRIO-2 orbit determination. His proposal took place independently of quite similar suggestions by Pisa University or ESA people.